JOURNAL OF CHEMICAL RESEARCH 2010 OCTOBER, 589–595 **RESEARCH PAPER** 589

Effect of thermal treatment of MCM-41 on the nature and catalytic properties of MCM41-supported alkoxo-titanium species in oxidation of sulfides to sulfoxides

Ilyes Khedher* and Abdelhamid Ghorbel

Laboratoire de Chimie des Matériaux et Catalyse. Département de Chimie. Faculté des Sciences de Tunis, 1060 Tunis, Tunisie

Titanium tetra-isopropoxide reacts with the silanol groups of MCM41 calcined at two different temperatures, 550 and 750°C, to form well-defined surface organometallic species. For MCM41 calcined at 550°C, the amount of available silanol allows mainly the formation of the bipodal titanium complex, $(\equiv SiO)_2Ti(O^iPr)_2$, while calcination at 750°C leads to the formation of the monopodal titanium complex $\equiv SiO–Ti(O^iPr)_3$. Ti–MCM41$_{(750)}$ was found to be more active and selective in the oxidation of sulfides, compared to Ti–MCM41$_{(550)}$, and this can be attributed to the development of a large amount of tetrahedral isolated titanium (IV) which seems to be the active site in this reaction. In the asymmetric oxidation of sulfide by H_2O_2, Ti–MCM41$_{(750)}$ was found also more reactive than Ti–MCM41(550), since it develops the singly bonded titanium species, $\equiv SiO–Ti(O^iPr)_3$, which appears to be the chiral active site in this reaction.

Keywords: MCM-41, catalysis, synthesis, oxidation, sulfide, sulfoxide

Heterogeneous titanium catalysts are of considerable interest due to their activity in the oxidation of various substrates.[1] This property can be achieved either by dispersion of titanium in a silica matrix or by grafting of titanium precursors to a silica support. Several authors have compared the performance of the two types of solids, and the supported catalysts are recognised as being more efficient than those containing the titanium centres in the matrix structure.[2–4] The preparation of silica-supported titanium catalysts occurs via an esterification process between titanium precursor and the silanol groups of the silica surface. According to several studies of the reactivity of the silica with different transition metal complexes,[5–7] the change of the density of the available surface Si–OH groups can affect the nature of the resulting titanium surface species. Indeed, the titanium centre can be bonded to one, two, or even three silicon atoms through Si–O–Ti bonds, leading to the formation of monopodal, bipodal, or tripodal species, respectively (Fig. 1), depending on the density of silanol groups on the surface.

Here, we investigate how changes in the nature and the overall concentration of the surface Si–OH groups can affect the nature of the resulting surface species. A simple way to modify the surface of silica consists of calcination at different temperatures. We now report a study of the effect of thermal treatment of the mesoporous silica MCM41 on the nature of the MCM41-supported alkoxo-titanium species. Two distinct Ti–MCM41 samples are described which were prepared from the impregnation of MCM41 calcined at two different temperatures of 550 and 750°C, with titanium alkoxide solution. The solids obtained were characterised with different physicochemical techniques to obtain structural information about the grafted titanium species. The catalytic properties of the MCM41-supported alkoxo-titanium species were examined in the symmetric and asymmetric oxidation of sulfide to sulfoxide, and the combination of the structure information and the catalytic properties can establish the molecular structure–reactivity relationship of the grafted titanium centres in these catalytic materials.

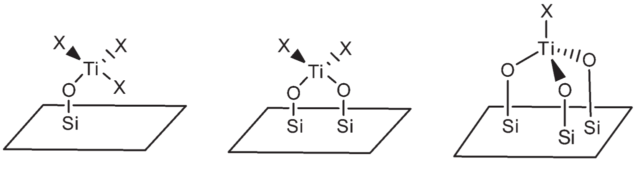

Fig. 1 Possible surface titanium species on silica.

Experimental

Synthesis

The synthesis of MCM41 used in this work had been described elsewhere.[8–9] Typically, MCM41 was prepared as follows: tetraethylorthosilicate (TEOS) was added to a mixture of acetyltrimethylammonium bromide ($C_{16}H_{33}Me_3NBr$, CTAB), ammonium hydroxide NH_4OH (Aldrich; 28% in H_2O) and H_2O. The molar composition of the above mixture was 1TEOS:0.2CTAB:8NH_4OH:114H_2O. This solution was stirred at 30°C for 1 h, then it was transferred into a polypropylene bottle and heated at 100°C for 72 h. The resulting solid product was filtered off, washed with de-ionised water, and dried at 50°C for 24 h. In order to remove the organic surfactant in the pores of MCM41, the as-synthesised samples were calcined in air at two different temperatures of 550 and 750°C for 6 h (using a heating rate of 1°C min^{-1}). These two calcined MCM41 species are referred to as MCM41$_{(550)}$ and MCM41$_{(750)}$.

Ti centres were grafted on to the surface of MCM41 by the incipient wetness impregnation method. Calcined MCM41 (0.5g) was activated by heating under vacuum at 120°C for 12h. To a mixture of activated solid and dry toluene (10 mL), was added $Ti(O^iPr)_4$ (1.25 mmol). The resulting mixture was stirred and heated under reflux under nitrogen gas for 24 h. The resulting solids were filtered and washed successively with dry toluene and diethyl ether, then dried under vacuum at ambient temperature. The dried material was subjected to Soxhlet extraction with dry dichloromethane for 24 h. Finally, the solids were dried at 50°C under vacuum for 8 h. The resulting materials are referred to as Ti–MCM41$_{(550)}$ and Ti– MCM41$_{(750)}$.

Characterisation

The MCM-41 samples were characterised by powder X-ray diffraction (XRD), UV-Vis, ^{29}Si– and ^{13}C MAS-NMR and BET surface area and porosity measurements. The XRD patterns were recorded on a Philips PW 1130/00/60 diffractometer using Ni-filtered CuK_α radiation and a Siemens goniometer. Solid-state ^{29}Si and ^{13}C MAS NMR spectra were obtained at room temperature using a Bruker MSL 400 spectrometer; For ^{13}C MAS NMR spectra, chemical shifts were referenced to external tetramethylsilane. N_2 adsorption–desorption isotherms were determined at 77 K on a Micrometrics ASAP 2000 apparatus using dinitrogen as the adsorbent. Samples were degassed at 373K for 5h before the measurements were obtained. The pore size distribution curves were obtained from analysis of the desorption branch of the isotherm by the BJH (Barrett-Joyner-Halenda) method. UV-Vis reflectance spectra were measured at room temperature with a Perkin-Elmer Lamda 8 instrument with $BaSO_4$ as reference. Elemental analysis of carbon was carried out on a Perkin-Elmer analyser. The Ti loading was estimated by atomic absorption spectrometry on a Perkin-Elmer 3100 apparatus, after sample dissolution by acid attack.

Catalytic test

The catalytic properties of Ti–MCM41 were tested in the oxidation of sulfide (1 mmol) to sulfoxide, which was performed by stirring the catalyst (0.05 mmol as Ti) in the presence of 1 mmol of oxidant in

---

* Correspondent. E-mail: ilyeskhadher@yahoo.com

dry dichloromethane (DMC) under an inert atmosphere, followed by the addition of the sulfide. The reaction was monitored by gas chromatography (SPB™-5 Capillary, 30m × 0.25mm × 0.25µm).

Results and discussion

The low-angle XRD patterns of MCM41 samples (with and without titanium) are shown in Fig. 2. The XRD patterns recorded on untreated $MCM41_{(550)}$ and $MCM41_{(750)}$ samples match well with those of the silica MCM-41 plymorph reported by Chen *et al.*[10] This indicates that the hexagonal structure of MCM41 is preserved after the increase of the calcination temperature from 550°C to 750°C. In the hexagonal *P*6*m* space group, the three major reflections, (100), (110) and (200), occur within the range 2–5° (2θ). The (100) line, easily detected with all samples, has been used to obtain the approximate unit-cell *a* parameters estimated on the basis of Eqn (1) ($a = 2d_{100} / \surd 3$) (Fig. 3).

Although small uncertainties in low diffraction angle values lead to non-negligible variation in d-spacing values, general trends can be observed from these estimates. First, the *a* unit-cell parameter of MCM41calcined at 750°C is smaller than that of MCM-41calcined at 550°C (compare Figs 2a and 2b). The increase of thermal treatment indicates a lattice contraction of the silica matrix of about 0.6 Å (see Table 1). According to the work reported by Chen *et al.*[10], this contraction can be explained by the condensation of Si–OH groups to generate the formation of cyclic trisiloxanes, as schematically indicated in Fig. 4. This is in good agreement with the decrease in silanol density showed below by ^{29}Si MAS NMR.

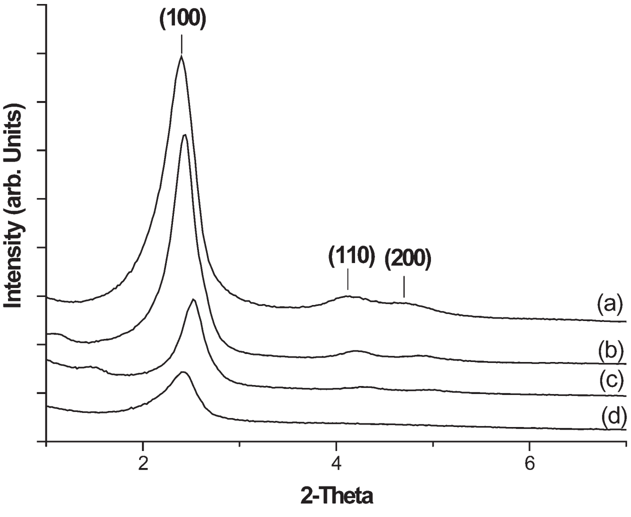

Fig. 2 XRD patterns of MCM41 samples: (a) $MCM41_{(550)}$, (b) $MCM41_{(750)}$, (c) Ti– $MCM41_{(550)}$ and (d) Ti– $MCM41_{(750)}$.

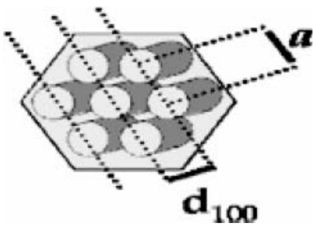

Fig. 3

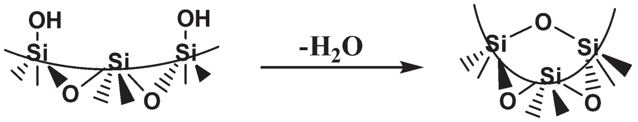

Fig. 4

When toluene $Ti(O^iPr)_4$ solution reacted with pure MCM41, the main peak intensity decreased in Ti–MCM41 samples (Figs 2c and 2d). This result suggests that the introduction of Ti species into the channel of MCM41 leads to a substantial loss in scattering contrast between the channel and the wall, and then reduces the intensity of the scattered X-ray in the powder diffraction experiment.[11] The introduction of Ti species into the channel generates also the disappearance of the two others smaller diffraction peaks (100) and (200), indicating a loss of the long-range regularity of the hexagonal arrays of mesopores of MCM41.[12–14] The presence of the Ti species inside the channels of MCM41 reveals that the unit-cell *a* parameter remains constant in Ti– $MCM41_{(750)}$ sample but decreases significantly in the Ti–$MCM41_{(550)}$ sample. This decrease suggests that, in the case of Ti–$MCM41_{(550)}$ sample, there are interactions between Ti centres and the silicate walls which are stronger than those in the case of Ti–$MCM41_{(750)}$ sample.

In addition, in the high angle region of XRD patterns, we note, in both the Ti–$MCM41_{(550)}$ and Ti–$MCM41_{(750)}$ samples, the absence of the diffraction peak corresponding to the bulk TiO_2 ($2\lambda = 25.5$), which is a good indication that the titanium was well dispersed within silica channels. This supposition is supported by UV-Vis study (Fig. 9). In fact, no band adsorption corresponding to anatase was detected.

The N_2 adsorption–desorption isotherms and the corresponding BJH pore size distributions based on the desorption branch for the MCM41 samples are shown in Figs 5 and 6. All the samples give similar adsorption–desorption isotherms of N_2. The nitrogen isotherm of $MCM41_{(550)}$ sample follows the type-IV isotherm with a sharp capillary condensation step at a relative pressure between 0.2 and 0.4, indicating a typical mesoporous structure with uniform pores.[15–17] By increasing the calcination temperature of MCM41 from 550 to 750°C, the sharp capillary condensation step shifts toward the low p/p_0 region, indicating a change in the pore structure (compare Figs 5a and 5b). According to X-ray diffraction, this change is due to a significant decrease of the pore-size by the condensation of surface Si–OH groups (see Table 1).

Compared to the untreated MCM41 samples, the pore structure is more affected in the cases of Ti–MCM41 samples (Figs 5c and 5d). This can be observed more clearly in Table 1. The introduction of titanium into the channels of MCM41 leads to a decrease of surface area and pore volume while wall thickness, estimated on the basis of Eqn (2) [$\delta = (a - D)$], increases. This could be explained by the filling of the pores with titanium species which remain bonded to the silica surface inner and increase the wall thickness. Consequently, the meso-channels became narrow and the pore diameter of the incorporated MCM-41 samples would also decrease, accompanying the decrease of

Table 1 Some structure parameters of the prepared materials

Samples	$MCM41_{(550)}$	$MCM41_{(750)}$	Ti–$MCM41_{(550)}$	Ti–$MCM41_{(750)}$
Ti loading ($mmol.g^{-1}$)	–	–	1.12	1.23
d_{100} (nm)	3.69	3.64	3.48	3.63
a (nm)[a]	4.26	4.20	4.01	4.19
Pore diameter (D) (nm)[b]	2.73	2.56	2.44	2.48
Wall thickness (δ) (nm)[c]	1.53	1.64	1.57	1.71
Surface area ($m^2\ g^{-1}$)	1230	920	742	611
Pore volume ($cm^3\ g^{-1}$)	0.81	0.65	0.33	0.22

[a] Calculated according to $a = 2\ d_{100} / \surd 3$ [Eqn (1)]

[b] The pore diameter was determined from the analysis of the desorption branch of the isotherm by the BJH (Barrett–Joyner–Halenda) method.

[c] Estimated according to $\delta = (a - D)$ [Eqn (2)]

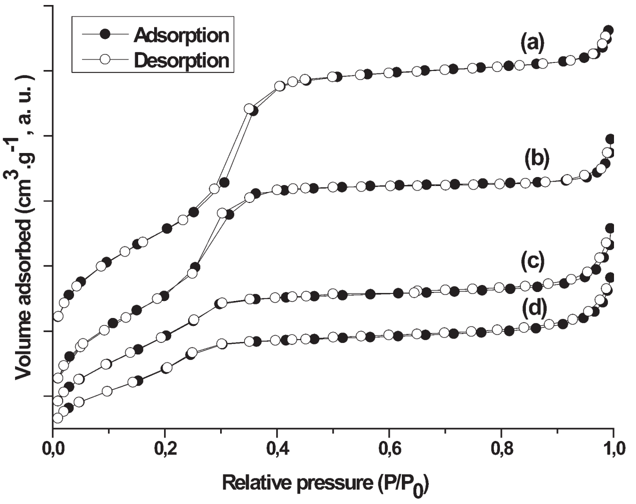

Fig.5 The nitrogen adsorption-desorption isotherms of MCM-41 samples: (a) MCM41$_{(550)}$, (b) MCM41$_{(750)}$, (c) Ti–MCM41$_{(550)}$ and Ti–MCM41$_{(750)}$.

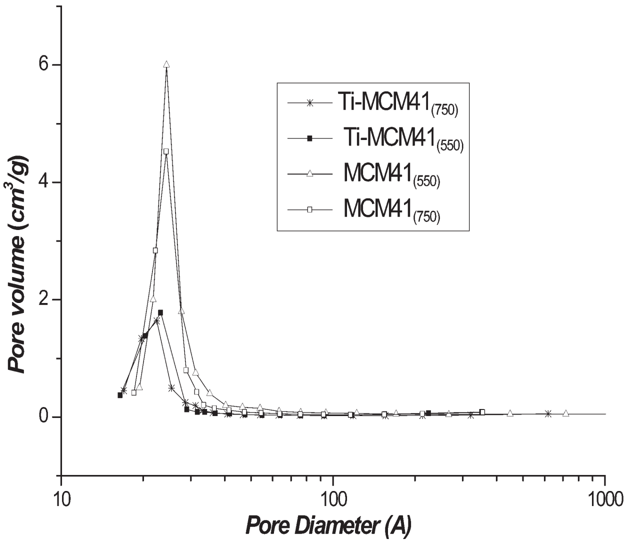

Fig. 6 BJH pore size distribution curve of MCM41$_{(550)}$, MCM41$_{(750)}$, Ti–MCM41$_{(550)}$ and Ti–MCM41$_{(750)}$ calculated from the desorption branch.

the pore volume and the surface area. As can be seen in Table 1, this effect is more pronounced in the case of the Ti–MCM41$_{(550)}$ sample, indicating a decrease of about 3Å in the average pore diameter. This observation correlates well with the decrease of the unit-cell *a* parameter showed by X-ray diffraction.

To summarise, the bulk characteristics of the Ti–MCM41 samples are comparable but not identical to those of calacined MCM41 supports. BET also reveals that, in the presence of titanium, the mesoporous channels remain accessible. However, the main pore diameter decreases significantly (Table 1 and Fig. 6). This last observation suggests that Ti species are located inside the channels, coating the walls of the mesoporous matrix Finally, a significant decrease of the unit-cell *a* parameter is observed in the case of Ti–MCM41$_{(550)}$ sample after titanium introduction and indicates strong interaction between Ti centres and the mesoporous walls. The presence of Ti species, multiply coordinated *via* (Si–O–Ti) bridges to the walls, could explain this last observation. Indeed, some pore-size shrinking, associated with *a* unit-cell decrease, could be expected if the Ti species are bonded to two (type B) and/or three (type C) Si–O groups and tend to curve the silica walls, as schematically indicated in Fig. 7. In contrast, the Ti species introduced into the channels of Ti– MCM41$_{(750)}$ sample are not expected to change the unit-cell *a* parameter significantly. The combination of this observation with the low number of available surface

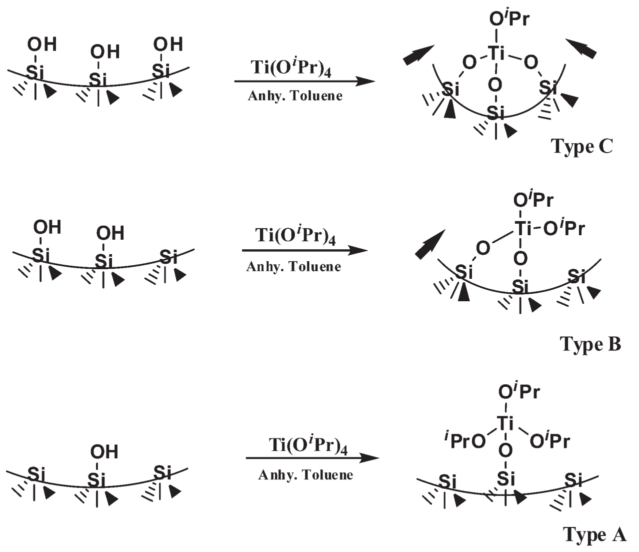

Fig. 7 Coordination of Ti centres on the mesoporous walls. Ti centres of type B and type C, coordinated by two and three (Si–O–Ti) bridges to the mesoporous walls are expected to change the pore curvatures. By contrast, the Ti centres of type A, only coordinated by one (Si–O–Ti) bridge to the walls, are not expected to change significantly the unit-cell ***a*** parameter.

silanol groups in the MCM41$_{(750)}$ sample, suggests that, in the case of Ti– MCM41$_{(750)}$, the titanium centre is probably bonded to one silicon atom through one Si–O–Ti bond (type A, Fig. 7).

In order to gain insight into the coordination of Ti centres on the mesoporous walls, ^{29}Si MAS-NMR investigations and chemical analysis have been undertaken. The ^{29}Si MAS-NMR technique is able to detect and in the same time to distinguish the three different silicon atoms that constitute the silica framework. It is worth noting that the silica framework is constituted of silicon atoms without hydroxyl groups Si–(Si–O)$_4$, silicon atoms bearing one hydroxyl group (Si–O)$_3$-Si–OH and silicon atoms bearing two hydroxyl groups (Si–O)$_2$-Si–(OH)$_2$ called geminal silanols. The (Si–O)$_2$-Si–(OH)$_2$ and (Si–O)$_3$-Si–OH species are present at the silica surface, while the Si–(Si–O)$_4$ species are present in the bulk.[18] The ^{29}Si MAS-NMR spectrum of MCM41$_{(550)}$ (Fig. 7a), is due to convolution of three peaks. The first peak, Q^2, centred at around -90 ppm, is due to the contribution of geminal silanols, the second peak, Q^3, at around –100 ppm, is due to the silicon atoms bearing one hydroxyl group and the third peak, Q^4, at around –109 ppm, is due to the silicon atoms without hydroxyl groups.[18] By the increase of thermal treatment from 550°C to 750°C, it is worth noting that the Q^2 area does not change significantly, whilst the Q^4 and Q^3 areas increase and decrease, respectively (compare Figs 8a and 8b). The MCM-41 structure modification is probably due to the condensation of the hydroxyl groups Q^3 (about 50%, see Table 2, entry 2) to form cyclic trisiloxane groups according to the data reported by Chen *et al.*[10] The amount of Q^2 stays roughly the same but the amount of Q^3 also decreases significantly when the Ti(O^{i}Pr)$_4$ reacts with the calcined MCM41 matrix, indicating the probable conversion of the (Si–O)$_3$–Si–OH groups into (Si–O)$_3$-Si–O–Ti groups (Table 2, entry 2).

Compared to Ti–MCM41$_{(550)}$, the titanium content in the case of Ti–MCM41$_{(750)}$ is higher, although it exhibits a lower number of available silanols groups (Table 2, entry 4). This would suggest that the amount of the Ti species grafted is more limited by steric hindrances than by any lack of available Si–OH groups. Consequently, the conversion of the (Si–O)$_3$-Si–OH groups in (Si–O)$_3$–Si–O–Ti groups is more pronounced in the Ti–MCM41$_{(750)}$ sample than in Ti–MCM41$_{(550)}$ sample (Table 2, entry 4).

However, the amount of isopropoxy ligands still bound to the metal centre of the surface species can be estimated by the quantification of the carbon-to-titanium ratio obtained by elemental analysis (Table 1, entry 6). This quantity increases with the decrease of available surface Si–OH groups (Table 1, entry 7). Ti–MCM41$_{(750)}$ gave around 3.4 isopropoxy groups per grafted titanium, indicating an average of three isopropoxy groups still bound to the Ti centre of the surface species

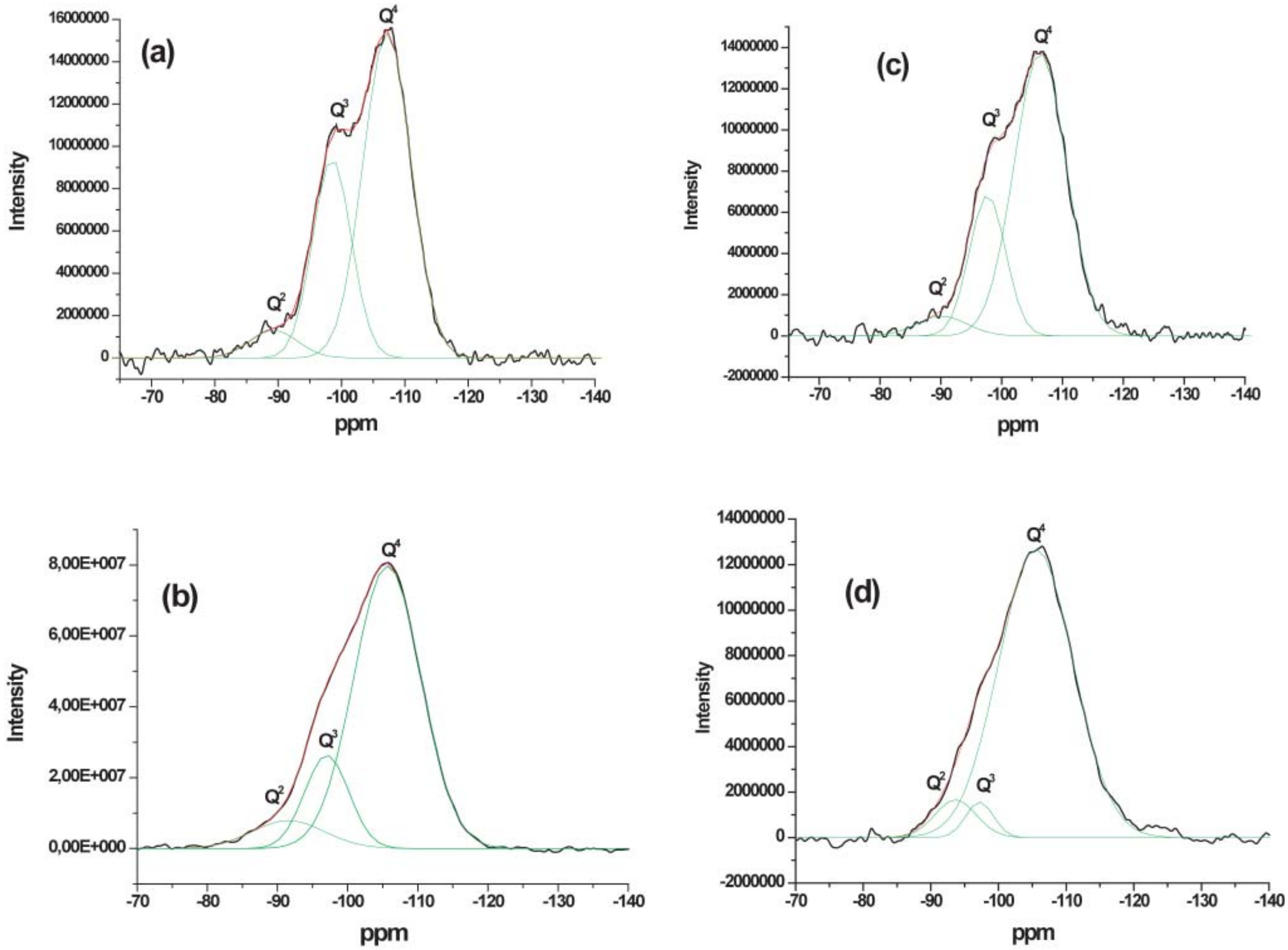

Fig. 8 ^{29}Si MAS-NMR spectra (lines) of MCM-41samples: (a) MCM41$_{(550)}$, (b) MCM41$_{(750)}$, (c) Ti–MCM41$_{(550)}$ and (d) Ti–MCM41$_{(750)}$. Peaks deconvolution (fit results: red line; single Gaussian: green lines).

Table 2 Coordination of Ti centres on the mesoporous walls

Entry	(1)	(2)	(3)	(4)	(5)	(6)	(7)
Samples	Q^2/mol %^{a}	Q^3/mol %^{a}	Q^4/mol %^{a}	Ti loading / mmol g^{-1}	Elem. Anal. C / mmol g^{-1}	C / Ti	Isopropoxy ligand /Ti
MCM41$_{(550)}$	5.4	31.3	63.3	–	–	–	–
MCM41$_{(750)}$	7.0	16.4	76.6	–	–	–	–
Ti–MCM41$_{(550)}$	4.9	24.3	70.8	1.12	8.38	7.50	2.5
Ti–MCM41$_{(750)}$	6.6	4.4	89.0	1.23	12.55	10.20	3.4

[a] Q^n (mol%) estimated by integration of peaks areas obtained by Gaussian deconvolution of the ^{29}Si MAS-NMR spectra

(theory: 3.0 for the coordination of type A, Fig. 7). From the XRD study, this result suggests that the monografted complex of type A (Fig. 7) is probably the main product on the surface. On the other hand, the bi-grafted complex (type B, Fig. 7) seems to be the main product formed on Ti–MCM41$_{(550)}$ since around 2.5 isopropoxy groups per grafted titanium were detected. From these results, the formation of tripodal titanium species can be discarded. The small excess of carbon showed by elemental analysis (isopropoxy ligand /Ti = 2.5 instead of 2 and 3.4 instead of 3 in the presumed SiO–Ti(O^{i}Pr)$_2$ and SiO–Ti(O^{i}Pr)$_3$, respectively), can be attributed to a few isopropanol molecules [the product of the exchange reaction between Ti(O^{i}Pr) and OH in the inner surface] H-bonded to residual silanols or coordinated to titanium alkoxide surface complexes. Indeed, the ^{13}C MAS-NMR spectra of Ti–MCM41$_{(550)}$ and Ti–MCM41$_{(750)}$ display three peaks at 26, 62 and 75ppm. The peak at 26 ppm can be attributed to the methyl carbon, while the two signals at 62 and 75ppm correspond to the ternary carbon atom O–*C*H– of isopropoxy-groups. The presence of these two peaks shows that two species exist on the surface. The signal at 75 ppm is attributed to the ternary carbon of isopropoxy ligands coordinated on Ti, ≡Ti–O*C*H(CH$_3$)$_2$, and the signal at 62 ppm to the ternary carbon of the isopropanol molecules HO–*C*H(CH$_3$)$_2$ (the product of the reaction between Ti(O^{i}Pr) and surface silanols groups) remaining physisorbed on the surface.[19]

The UV-Vis spectra of both Ti–MCM$_{(550)}$ and Ti–MCM$_{(750)}$ show an intense band centred at 259nm together with another less intense band at 223 nm. The band at 259 nm is due to the electronic transition from O^{2-} to Ti^{4+}. Similar high-energy absorption edges due to isolated penta- and hexa-coordinated Ti(IV) atoms have been observed for other titanium-containing mesoporous molecular sieves.[20] The band at 223 nm corresponds to tetrahedrally-coordinated titanium in an isolated state.[21,22] Absence of a 330 nm peak for both samples indicates that no bulk titania is formed. These results can be taken as a parameter which shows the high dispersion of Ti species in MCM41.

From the convolution of two bands, it is worth noting that the amount of titanium in tetrahedral coordination is much greater in the case of Ti–MCM$_{(750)}$ than in the case of Ti–MCM$_{(550)}$. This allows us to

Table 3 Oxidation of methyl phenyl sulfide catalysed by Ti–MCM41 samples

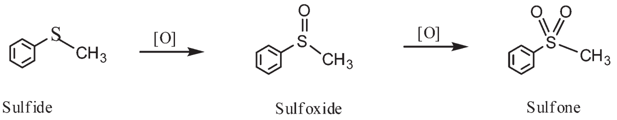

Entry	Catalyst	Oxidant	Conversion /%	Sulfoxides /%	Sulfone /%
1	None	CHP	6	>99	0
2	MCM41$_{(550)}$	CHP	4	>99	0
3	MCM41$_{(750)}$	CHP	5	>99	0
4	Ti–MCM41$_{(550)}$	CHP	64	85	15
5	Ti–MCM41$_{(550)}$	H_2O_2	41	62	38
6	Ti–MCM41$_{(750)}$	CHP	73	87	13
7	Ti–MCM41$_{(750)}$	H_2O_2	53	67	33

Reaction conditions: Methyl phenyl sulfide, 1 mmol; catalyst, 0.05 mmol as Ti; oxidant, 1 mmol; CH_2Cl_2 10 mL; 293K; 4h.

deduce that the increase of deshydroxylation effect appears a favourable factor for the formation of surface species in low coordination (tetrahedral).

In addition, the increase in the coordination of the titanium from tetra- to penta- and hexa-coordinated might be due to intermolecular interactions with siloxane groups [23] or with residual isopropanol molecules, (the product of the exchange reaction between Ti(O^{i}Pr) and OH in the inner surface), detected by ^{13}C MAS-NMR.

Catalytic oxidation of sulfide on Ti–MCM41

The above results prompted us to study Ti–MCM41$_{(550)}$ and Ti–MCM41$_{(750)}$ as oxidation catalysts and the selective oxidation of sulfide to sulfoxide was selected as the benchmark reaction. The results obtained using thioanisole as sulfide are given in Table 3. As can be seen, in the absence of catalyst (entry 1) or in the presence of MCM41$_{(550)}$ or MCM41$_{(750)}$ as catalyst (entries 2 and 3) the reaction is very slow, but in the presence of Ti–MCM41$_{(550)}$ or Ti–MCM41$_{(750)}$ most of the substrates are oxidised to give high yields.

The possibility of homogenous catalysis by titanium ions leaching from the Ti–MCM41$_{(550)}$ and Ti–MCM41$_{(750)}$ catalysts has been investigated. To accomplish this, the reaction was conducted under similar reaction conditions and then stopped after 30 min. The hot liquid medium was removed with a syringe equipped with a filter and immediately transferred to another reactor maintained at the same temperature. The compositions were then monitored over another 1.5 h. No activity was found in the liquid phase alone. This blank experiment indicates that no Ti species had leached out of the catalyst and that the oxidation reaction was stopped after catalyst removal, indicating that the activity of the catalyst can only be due to the Ti atoms incorporated onto the surface of the silica support.

The results given in Table 3 show also that Ti–MCM41$_{(750)}$ is more active and selective towards the formation of sulfoxide than Ti–MCM41$_{(550)}$, particularly when CHP was used as oxidant, which seems to be more efficient in the oxidation of sulfide than H_2O_2. This is not surprising in view of the fact that CHP is an active oxidant in the homogenous and heterogenous oxidation reactions.[24–26] The high catalytic activity of the Ti–MCM41$_{(750)}$ sample is probably attributable to the presence of a proportion of tetrahedral isolated titanium detected by UV-Vis spectroscopy, which is more important in the case of Ti–MCM41$_{(750)}$ than in Ti–MCM41$_{(550)}$. In fact, it is now generally accepted that the active site of this type of catalyst (oxide-supported titanium complexes and titanium silicates) involves isolated open sites, that is, tetrahedral isolated titanium (IV) centres linked to the surface by siloxy bridges.[27]

Asymmetric oxidation of sulfide on Ti–MCM41

Chiral titanium complexes have proved to be useful catalysts in several asymmetric oxidations.[28–31] This fact, together with the usefulness of optically active sulfoxides in asymmetric synthesis of organic compounds, prompted us to study the effect of a chiral modifier on the Ti–MCM41catalysts. The chiral modifier used is a Schiff base ligand (**1**). It has been shown that the Schiff base ligand is able to coordinate many different metals, and to stabilise them in various oxidation states, enabling the use of Schiff base metal complexes for a large variety of useful catalytic transformations such as asymmetric epoxidation [32–34] and asymmetric sulfide oxidation.[24–25,35] The results obtained in the asymmetric oxidation of methyl phenyl sulfide are listed in Table 4.

It can be seen that the addition of the chiral modifier causes reduced catalytic activity of both catalysts. This indicates that the chiral modifier is probably coordinated to the catalytic centres. In contrast, only the Ti–MCM41$_{(750)}$ sample shows a low but significant enantioselective catalytic activity. This can be explained by its development of the singly bonded titanium species ≡SiO–Ti(O^{i}Pr)$_3$ which seems to be easily accessible and coordinate to the chiral modifier and oxidant leading to a chiral active site for this reaction (Fig. 10, complex **A**). Indeed, from the homogeneous catalytic process reported by Kagan *et al.*[29–31] in the asymmetric oxidation of sulfide using a Ti(IV)/*DET* complex, it is usually accepted that the active titanium centre is coordinated, with the chiral ligand chelating the metal via two σ-bonded oxygen atoms and σ-π-coordinated *R*-peroxo ligand (Scheme 1, complex **2**). Thus if Ti (IV) is grafted *via* two ≡Si-O-Metal bonds, it cannot accommodate all these ligands, and is then an inactive site (Fig. 10, complex **B**) and /or an active but not enantioselective site (Fig. 10, complex **C**), while Ti(IV) grafted onto silica by one ≡Si–O–Ti can engage the three covalent bonds required leading to a chiral active site (Fig. 10, complex **A**). Additionally, the nature of the oxidant has a great influence on the selectivity and enantioselectivity of the reaction. Indeed, H_2O_2 as oxidant seems to be more active in the heterogenous asymmetric oxidation than CHP. This is surprising in

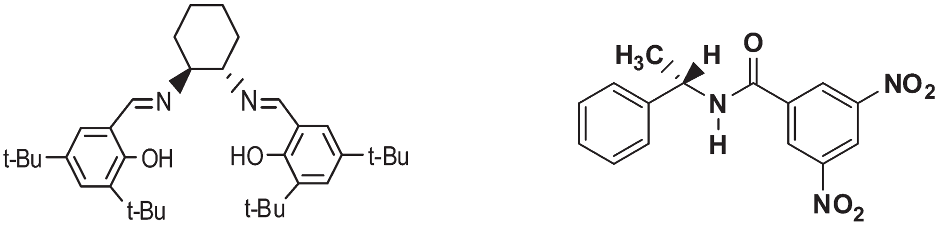

(1)

(2)

Fig. 9 Chiral Schiff base (**1**) and chiral shift reagent (**2**).

Table 4 Results obtained in the asymmetric oxidation of methyl phenyl sulfide

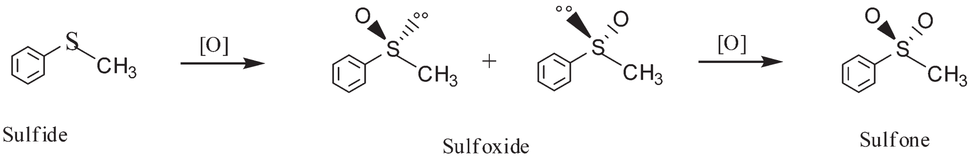

Catalyst	Oxidant	Conversion /%	Sulfoxide /%	Sulfone /%	ee /%
Ti–MCM41$_{(550)}$	CHP	31	42	58	0
Ti–MCM41$_{(750)}$	CHP	34	74	26	5
Ti–MCM41$_{(550)}$	H_2O_2	46	86	14	0
Ti–MCM41$_{(750)}$	H_2O_2	47	91	9	10

Reaction conditions: Methyl phenyl sulfide, 1 mmol; Catalyst, 0.05 mmol as Ti; oxidant, 1 mmol; CH_2Cl_2 10 mL; chiral modifier/Ti = 1:1.
The ee's were determined from the ^{1}H NMR spectrum in the presence of the chiral shift reagent **(2)**.

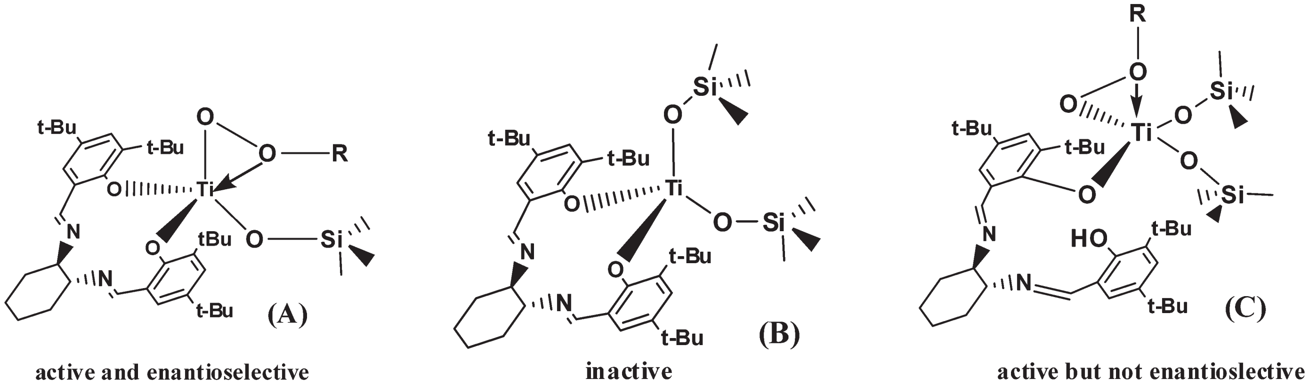

Fig. 10

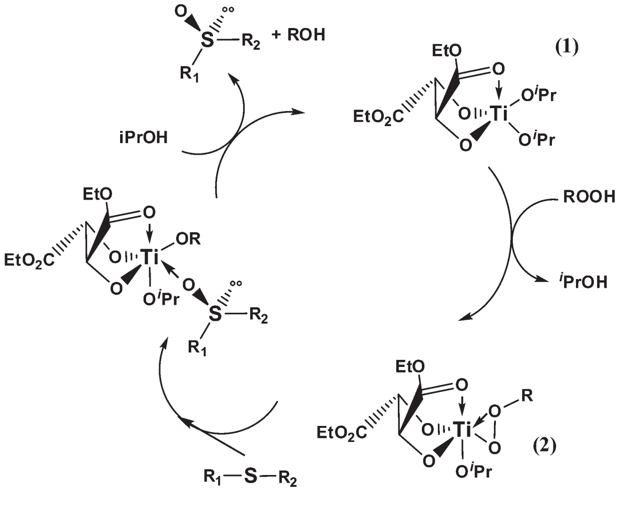

Scheme 1 Enantioselective sulfide oxidation with Ti(IV)/DET complexes.

view of the fact that CHP is an active oxidant in homogenous asymmetric oxidation.[24–25] This is probably due to the difference between the properties of active sites on the surface and in the solution; the bulky phenyl group of CHP would interfere with the appropriate coordination of chiral ligands with titanium ions in the pores.

Conclusion

The present study demonstrates that ultra-large pore materials containing highly dispersed Ti centres and having a hexagonal MCM41 structure can be synthesised by grafting. Combined spectroscopic (^{29}Si– and ^{13}C MAS-NMR and UV-Vis), bulk structural characterisations (X-ray diffraction, BET) and chemical assays show that for a silica calcined at 550°C, the amount of available silanols allows the formation of, mainly, a bi-grafted titanium complex, $(\equiv SiO)_2Ti(O^iPr)_2$ while calcination at 750°C leads to the formation of a monopodal titanium complex, $\equiv SiO–Ti(O^iPr)_3$. The change of the density of available silanol groups on the silica surface thus constitutes a way to control the hapticity of silica towards organometallic complexes. In both samples, two different titanium species have been identified by UV-Vis spectroscopy, the first is an isolated penta- or hexa-coordinated Ti(IV) atom and the second is Ti(IV) in an isolated tetrahedral environment, which seems to be the catalytic site that readily interact with oxidant to offer an active and selective catalytic system for the oxidation of sulfides. The latter makes the catalytic activity of Ti–MCM41$_{(750)}$ higher than that of the Ti–MCM41$_{(550)}$. Indeed, Ti–MCM41$_{(750)}$ develops a larger amount of tetrahedral, isolated titanium (IV) than does Ti–MCM41$_{(550)}$. Ti–MCM41$_{(550)}$ and Ti–MCM41$_{(750)}$, when modified by a chiral ligand, show reduced catalytic activity in the oxidation of methyl phenyl sulfide. Only Ti–MCM41$_{(750)}$ leads to a low but significant enantioselective catalytic activity, which can be due to its development of a monopodal titanium complex, $\equiv SiO–Ti(O^iPr)_3$, which seems to be a chiral active site in this reaction, mainly with the use of H_2O_2 as oxidant.

Received 10 June 2010; accepted 26 August 2010
Paper 1000188 doi: 10.3184/030823410X12867300849443

References

1 R.A. Sheldon, M. Wallau, I.W.C.E. Arends and U. Schuchardt, *Acc. Chem. Res.*, 1998, **31**, 485.
2 R.D. Oldroyd, J.M. Thomas, T. Maschmeyer, P.A. MacFaul, D.W. Snelgrove, K.U. Ingold, and D.D.M. Wayner, *Angew. Chem. Int. Ed.*, 1996, **35**, 2787.
3 L.Y. Chen, G.K. Chuah and S. Jaenicke, *Catal. Lett.*, 1998, **50**, 107.

4 M.S. Morey, S. O'Brien, S. Schwarz and G.D. Stucky, *Chem. Mater*., 2000, **12**, 898.
5 L. Lefort, M. Chabanas, O. Maury, D. Meunier,C. Copéret, J. Thivolle-Cazat and J.-M. Basset, *J. Organomet. Chem*., 2000, **593**, 96.
6 V. Riollet, M. Taoufik, J.-M. Basset and F. Lefebvre, *J. Organomet. Chem*., 2007, **692**, 4193.
7 R. Petroff Saint-Arroman, B. Didillon, A. de Mallmann, J.-M. Basset and F. Lefebvre, *J. Organomet. Chem*., 2001, **625**, 101.
8 T. Asefa, M.J. Maclachlan, N. Coombs and G.A. Ozin, *Nature*, 1999, **402**, 867.
9 X. Hao, Y. Zhang, J. Wang, W. Zhou, C. Zhang and S. Liu, *Microporous Mesoporous Mater*., 2006, **88**, 38.
10 C.–Y. Chen, H.–X. Li and M. E. Davis, *Microporous Mater*., 1993, **2**, 17.
11 I. Kinski, H. Gies and F. Marlow, *Zeolite,* 1997, **19**, 375.
12 J.M.F.B. Aquino, A. S. Araujo, D. M.A. Melo, J. E.C. Silva, M. J.B. Souza and A.O.S. Silva, *J. Alloys Compd*., 2004, **374**, 101.
13 R. Kohn and M. Froba, *Catal. Today*, 2001, **68**, 227.
14 M. Froba, R. Kohn, G. Bouffaud, O. Richard and G. van Tendeloo*, Chem. Mater*., 1999, **11**, 2858.
15 S. Vetrive and A. Pandurangan, *Catal. Lett*., 2005, **99** (3–4), 141.
16 M. Ziolek, A. Lewandowska and B. Grybowska, *React. Kinet. Catal. Lett*., 2003, **80**, 199.
17 X. Gao, I.E. Wachs, M. Wong and J Ying, *J. Catal*., 2001, **203**, 18.
18 A. P. Legrand, *J. Chim. Phys*., 1987, **10**, 1204.
19 D. E. Babushkin and E. P. Taisi, *React. Kinet. Catal. Lett*., 1999, **67** (2), 359.
20 A. Corma, M. Iglesias and F Sánchez, *Catal. Lett*., 1996, **39**, 153.
21 M. Crocker, R.H.M. Herold, A.G. Orpen and M.T.A. Overgaag, *J. Chem. Soc., Dalton Trans*., 1999, 3791.
22 K. Wada, N. Itayama, N. Watanabe, M. Bundo, T. Kondo and T. Mitsudo, *Organometallics*, 2004, **23**, 5824.
23 J. M. Fraile, J. I. García, J. A. Mayoral and E.Vispe, *J. Catal*., 2005, **233**, 90.
24 K. Nakajima, K. Kojima, T. Aoyama and J. Fujita, *Chem. Lett*., 1986, 1483.
25 C. Sasaki, K. Nakajima, M. Kojima and J. Fujita, *Bull. Chem. Soc. Jpn*., 1991, **64**, 1318.
26 D. Meunier, A. de Mallmann, and J.-M. Basset, *Topics Catal*., 2003, **23** (1–4), 183.
27 J.K.F. Buijink, J.J.M. Van Vlaanderen, M. Crocker and F.G.M. Niele, *Catal. Today*, 2004, **93**, 199.
28 T. Katsuki and K.B. Sharpless, *J. Am. Chem. Soc*., 1980, **102**, 5974.
29 P. Piychen and H.B. Kagan, *Tetrahedron Lett*., 1984, **43**, 3135.
30 P. Pitchen and H.B. Kagan, *Tetrahedron Lett.*, 1984, **25**, 1049.
31 J.M. Brunel and H.B. Kagan, *Bull. Soc. Chim. Fr*., 1996, **133**, 1109.
32 G. Pozzi, F. Cinato, F. Montanari and S. Quici, *J. Chem. Soc. Chem. Commun*., 1998, 877.
33 H.-L. Shyu, H.-H. Wei, G.-H. Lee and Y. Wang, *J. Chem. Soc. Dalton Trans*., 2000, 915.
34 N.H. Lee and E.N. Jacobsen, *Tetrahedron Lett*., 1991, **32**, 6533.
35 B. Saito and T. Katsuki, *Tetrahedron Lett*., 2001, **42**, 3873.